

PAPER

Linear and nonlinear optical analysis on semiorganic L-proline cadmium chloride single crystal

To cite this article: Mohd Anis *et al* 2018 *Chinese Phys. B* **27** 047801

View the [article online](#) for updates and enhancements.

Related content

- [Influence of bis-thiourea nickel nitrate on the structural, optical, electrical, thermal and mechanical behavior of a KDP single crystal for NLO applications](#)
Y B Rasal, R N Shaikh, M D Shirsat *et al.*
- [Third harmonic generation and thermo-physical properties of benzophenone single crystal for photonic applications](#)
A Saranraj, S Sahaya Jude Dhas, G Vinitha *et al.*
- [Single crystal growth and enhancing effect of glycine on characteristic properties of bis-thiourea zinc acetate crystal](#)
Mohd Anis and G G Muley

Linear and nonlinear optical analysis on semiorganic *L*-proline cadmium chloride single crystal

Mohd Anis^{1,†}, M I Baig², S S Hussaini³, M D Shirsat⁴, Mohd Shkir^{5,6}, and H A Ghramh⁵

¹Department of Physics, Sant Gadge Baba Amravati University, Amravati-444602, Maharashtra, India

²Prof. Ram Meghe College of Engineering and Management, Amravati-444701, Maharashtra, India

³Crystal Growth Laboratory, Department of Physics, Milliya Arts, Science and Management Science College, Beed-431122, Maharashtra, India

⁴RUSA Center for Advanced Sensor Technology, Department of Physics, Dr. Babasaheb–Ambedkar–Marathwada University, Aurangabad-431005, Maharashtra, India

⁵Research Center for Advanced Materials Science (RCAMS), King Khalid University, P. O. Box 9004, Abha-61413, Saudi Arabia

⁶Advanced Functional Materials & Optoelectronic Laboratory (AFMOL), Department of Physics, College of Science, King Khalid University, P. O. Box 9004, Abha-61413, Saudi Arabia

(Received 3 November 2017; revised manuscript received 1 January 2018; published online 10 March 2018)

In the current investigation, *L*-proline cadmium chloride monohydrate (LPCC) single crystal is grown by a slow solvent evaporation technique to identify its credibility for nonlinear optical device applications. The constituent elements of LPCC crystal are determined by the energy dispersive spectroscopic (EDS) technique. The single crystal x-ray diffraction technique is used to determine the structural dimensions of LPCC crystal. The UV-visible studies are carried out within a wavelength range of 200 nm–1100 nm to determine the optical transmittance of LPCC crystal. The linear optical parameters of LPCC crystal are evaluated using the transmittance data to discuss its importance for distinct optical devices. The Nd:YAG laser assisted Kurtz–Perry test is carried out to determine the enhancement in second harmonic generation efficiency of LPCC crystal with reference to KDP crystal. The Z-scan technique is employed to assess the third order nonlinear optical (TONLO) properties of LPCC crystal at 632.8 nm. The Z-scan data are utilized to evaluate the TONLO refraction, absorption and susceptibility of LPCC crystal. The color oriented luminescence behavior of LPCC crystal is investigated within a spectral range of 350 nm–700 nm. The dependence of dielectric constant and dielectric loss on temperature and frequency is evaluated through the dielectric measurement studies.

Keywords: crystal growth, dielectric studies, nonlinear optical materials, optical studies

PACS: 78.20.Ci, 78.60.–b

DOI: 10.1088/1674-1056/27/4/047801

1. Introduction

The challenge of designing efficient nonlinear optical (NLO) crystal has gained huge pace over few decades. Interestingly, the unexplored new class of semiorganic complex crystal is still an amateur but rapidly progressing field, which fascinates large audiences due to its bilateral contribution of properties associated with organic and inorganic counterparts. The coordination of organic and inorganic substrate reinforces acentric complex crystals, yielding a high nonlinear response.^[1–4] In the current era of advanced functional materials it is a thought provoking fact that amino acid assisted organic-metal complex crystals stand out amongst the large regime of semiorganic NLO crystals are subject to an abundance of typical features such as high threshold to laser damage, large nonlinear response, low angular sensitivity, extended donor-acceptor network and high mechanical hardness, which fetches its desirability for practical utility in photonics, optoelectronics, optical modulation, frequency conversion, optical data storage and telecommunication devices.^[5–8] As the presence of closed d¹⁰ shell elec-

trons in transition metals manifests a high optical response,^[9] hence the growth of promising amino acid metal complex (AAMC) crystal has been an innovative idea which is currently on the verge and actively involves many research groups of the current era. Several potential AAMC crystals exhibiting an appreciable linear and nonlinear optical response are *L*-alanine sodium nitrate (LASN),^[10] *L*-proline lithium bromide (LPLB),^[11] *L*-alanine potassium chloride (LAPC),^[12] *L*-valine cadmium chloride (LVCC),^[13] bis *L*-proline cadmium iodide (BLPC),^[14] *L*-alanine cadmium chloride,^[15] *L*-proline magnesium chloride,^[16] and *L*-proline cadmium chloride (LPCC).^[17–20] The literature reveals that the LPCC crystal is an interesting NLO crystal which needs to be investigated thoroughly for identifying its credibility for distinct device applications. The optimization of growth parameters brings out significant changes in characteristic properties of crystal. The literature survey on the growth of LPCC crystal at different temperatures: 45 °C,^[17] 27 °C,^[19] 40 °C^[20] reveals prominent changes in crystal growth, optical, dielectric, and mechanical properties. In the present study the growth tempera-

[†]Corresponding author. E-mail: loganees@gmail.com; loganees@yahoo.com

ture of LPCC crystal is optimized to 36 °C while an additional novelty is that the complete third-order nonlinear optical properties of LPCC crystal are firstly investigated at 632.8 nm in this paper. Thus a unique approach is adopted to explore the features of LPCC crystal by employing crystal growth, single crystal x-ray diffraction, energy dispersive spectroscopy, UV-visible study, SHG efficiency test, Z-scan, dielectric and fluorescence characterization techniques.

2. Experimental procedure

The AR grade raw material (*L*-proline and cadmium chloride) of purity 99% were purchased and recrystallized to eliminate the impurity at the primary stage of synthesis. The *L*-proline and cadmium chloride were later measured in stoichiometric ratio (1:1) and dissolved in double distilled water to allow the reaction for synthesis of *L*-proline cadmium chloride (LPCC) complex. The reaction mixture was allowed to agitate at a constant speed for six hours in order to facilitate homogeneous bonding. The reaction mixture was later filtered in a clean beaker through the membrane filter paper with the help of a vacuum pump. This beaker containing the filtered solution was covered with a porous sheet to avoid inclusion of dust particles and keenly placed in a constant temperature bath for slow evaporation at 36 °C. The seed crystals of LPCC were harvested within 10–12 days and the 21 mm × 10 mm × 0.7 mm bulk single crystal grown within a period of 20 days is shown in Fig. 1(a).

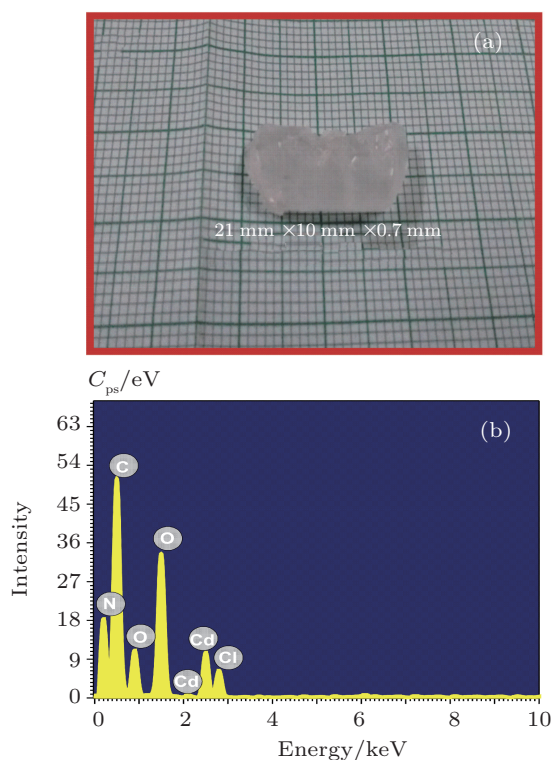


Fig. 1. (color online) (a) Single crystal of LPCC and (b) EDS spectrum of LPCC.

3. Results and discussion

The LPCC crystal is subjected to the single crystal XRD technique at room temperature using the Enraf Nonius CAD4 crystal diffractometer. The experimentally determined structural parameters of LPCC crystal are discussed in Table 1. The analysis of the data reveals that LPCC crystallizes with orthorhombic crystal symmetry and belongs to the noncentrosymmetric space group $P2_12_12_1$. The structural parameters are in good agreement with those presented in Ref. [17].

Table 1. XRD data.

Structural parameter	LPCC	LPCC ^[17]
Crystal system	Orthorhombic	Orthorhombic
Space group	$P2_12_12_1$	$P2_12_12_1$
$a/\text{Å}$	9.955	9.952
$b/\text{Å}$	13.479	13.484
$c/\text{Å}$	7.251	7.255
$V/\text{Å}^3$	972.96	973.60

The elemental analysis of LPCC crystal is assessed by the energy dispersive spectroscopic (EDS) technique using the Hitachi S4700 instrument. The single crystal of LPCC is powdered and the energy spectrum is traced in an energy range of 0 keV–10 keV. The energy peaks corresponding to the elements are indexed in the spectrum shown in Fig. 1(b). The analysis of the EDS spectrum reveals the presence of carbon (47.43%), nitrogen (19.43%), oxygen (21.23%), chlorine (3.72%), and cadmium (8.19%). This evidences the formation of LPCC crystal complex.

Optical analysis gives the clues of associated electronic band structures and compositional nature of the material.^[21,22] In the case of linear transmittance, the promotion of electrons to permitted energy states due to the absorption of incident photon and the inherent optical behavior of optically active functional units of the material are the principal parameters that determine the operative range of material in the optical spectrum.^[23–25] In addition, constraints associated with single crystal such as anisotropy in molecular alignment along the crystal plane and defects (voids, vacancies, grain boundaries, striations, pits, solvent impurities, inclusions) tune the intensity of optical transmittance.^[26–28] From the point of view of applications, the optical transmittances of NLO material in three prominent regions of spectrum far-UV (< 200 nm), visible (350 nm–700 nm) and NIR (ca. 1200 nm) need monitoring.^[29] In the present case the LPCC crystal (2-mm thickness) is scanned in a range of 200 nm–1100 nm using the spectrophotometer (Shimadzu-1601). The transmittance spectrum shown in Fig. 2(a) reveals that the LPCC crystal offers 84% transmittance which is uniform throughout the spectral range and the cutoff wavelength (λ_{cutoff}) is found to be at 232 nm. The observed high transmittance in

LPCC crystal might have been governed by the low absorption tendency of amino acid (*L*-proline in the present case) and the minimum density of defects which sustain the impediment of free propagation of light in a crystal medium. The LPCC crystal with high transmittance within 240 nm–1100 nm claims its potential candidature for efficient transmission of the second and third harmonic signal of Nd:YAG laser operative at 1064 nm.^[30] The transmittance of presently grown LPCC crystal is much superior to LPCC crystals grown at 45, 27, and 40 °C having transmittances of ~ 80%, ~ 60%, and ~ 50% respectively. The evaluated optical energy band gap ($E_g = 1243/\lambda_{\text{cutoff}}$)^[31] of LPCC crystal turns out to be 5.35 eV. The thorough knowledge of linear optical parameters of the single crystal is essential to scrutinize the material for distinct optical applications. Hence for the variations of optical conductivity (σ_{op} , Fig. 2(b)), extinction coefficient (K , Fig. 2(b)), refractive index (n , Fig. 2(c)), and reflectance (R , Fig. 2(b)) in the studied wavelength range are successfully evaluated using the formulae available in Ref. [32]. The anal-

ysis of graphs reveals that the optical conductivity and extinction coefficient increase with incident photon energy increasing. The LPCC crystal with high optical conductivity of the order of 10^{13} and extinction coefficient of the order of 10^{-5} possesses prerequisite qualities desirable for designing optical information processing and computing devices.^[33] The resistance to the propagating light wave in a medium causes the velocity of light to change, which gives birth to the vital optical parameter refractive index. The refractive index of LPCC crystal is significantly lower in a range of 300 nm–1100 nm and materials with lower refractive index are in high demand for fabricating optical memory storage media for high resolution holographic systems^[34] and calibrating the optical components (reflectors/filters/reflectors) used in solid state lasers.^[35] The solar thermal device needs the coating material that can trap more and reflect less light incident on it and therefore the lower magnitude of reflectance throughout the visible region makes it a potential candidate as antireflecting coating material for solar thermal devices.^[36]

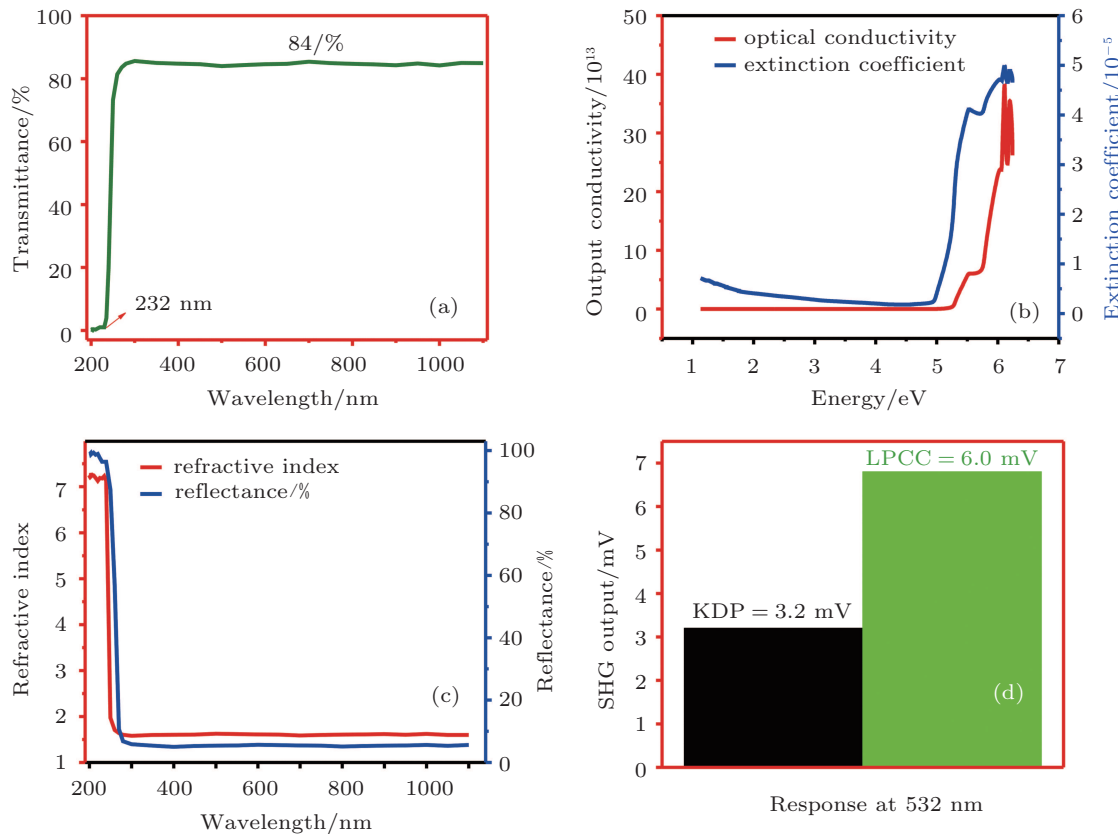


Fig. 2. (color online) (a) UV-visible transmittance spectrum, (b) variation of optical conductivity and extinction coefficient, (c) variation of refractive index and reflectance, and (d) graphical representation of SHG response.

Crystals with high conversion efficiency are largely demanded by the photonic industry, hence the occurrence of the frequency doubling phenomenon in LPCC crystal has been experimentally determined using the Kurtz–Perry powder SHG efficiency test.^[37] For sampling, all the components are aligned and the Nd:YAG laser (1064 nm, 8 ns, 10 Hz) is

tuned to the Q-switched mode. The powder samples of LPCC and potassium dihydrogen phosphate (KDP) material are prepared and tightly packed in the microcapillary tube. Each sample is independently irradiated multiple times by the Gaussian filtered beam of laser and the output window is monitored. The emergence of green light is confirmed and the out-

put signals are collimated through an array of photomultiplier tubes and further converted into an electrical signal to be displayed on an oscilloscope. The recorded voltages for KDP and LPCC crystal are shown in Fig. 2(d). The SHG efficiency of LPCC crystal is thus found to be 2.12 times higher than that of KDP. The high magnitude of SHG efficiency of LPCC crystal might be due to (i) the fact that the structural disordering/discrepancy in semiorganic molecular crystals leads to the formation of a sub-energy band below the energy gap, which increases the electron-phonon interaction and thus facilitates the favorable surrounding for photoinduced nonlinear optical effects to dwell efficiently,^[38] and (ii) the enhanced charge transfer induced by the metal-organic coordination (donor-acceptor bridge). The SHG efficiency of LPCC crystal is higher than LPLB (0.3 times that of KDP),^[11] LPZC (0.5 times that of KDP), and BPCI (twice that of KDP)^[14] crystals. Thus LPCC crystal with high SHG efficiency is a competent alternative for designing frequency converters and SHG device elements.^[39,40]

The focused beam irradiation of high intensity on the crystal surface dwells in an anharmonic manner in energy distribution due to which several third-order nonlinear optical effects evolve. The third order nonlinear optical (TONLO) effects are very sensitive and therefore accountability of the Z-scan technique is much higher for examining these TONLO properties of the given substrate. The Z-scan technique was proposed first by Bahae *et al.*^[41] The configuration of Z-scan setup used for analysis is detailed in Table 2.

Table 2. The optical resolution of Z-scan setup.

Parameters and notations	Details
Laser wavelength λ/nm	632.8
Lens focal length f/mm	30
Optical path distance Z/cm	85
Beam waist radius ω_a/mm	3.3
Aperture radius r_a/mm	2
Incident intensity at the focus $I_0/\text{KW}/\text{m}^2$	2.3375

The trace of TONLO refraction (n_2) in LPCC crystal is trailed using the closed aperture Z-scan analysis. To start the analysis, the He-Ne laser was optically aligned and the Gaussian filtered laser beam was converged via convex focusing lens to make localized irradiation on the crystal sample positioned at focus ($Z = 0$). The crystal is translated along the beam irradiated path, i.e., the Z direction which is equally divided into two halves with focus as the midpoint. The contributed change in transmitted light about the focus is monitored through the photo detector placed at the far field. The on-axis phase shift in TONLO refraction is governed by spatial distribution of energy along the crystal surface due

to a localized thermal lensing effect^[42] and it can be effectively tuned by modifying the repetition rate of the incident beam.^[43,44] The closed aperture Z-scan transmittance curve shown in Fig. 3(a) depicts that the pre-focus peak followed by post-focus valley resembles the feature of negative nonlinear refraction which is the inherent characteristic of material possessing self-defocusing tendency.^[45,46] The LPCC crystal with self-defocusing nature could be adopted for designing optical night vision sensor devices.^[47] The peak-to-valley transmittance (ΔT_{p-v}) and on-axis phase shift ($\Delta\phi$) are related by^[41]

$$\Delta T_{p-v} = 0.406(1 - S)^{0.25} |\Delta\phi|, \quad (1)$$

where $S = [1 - \exp(-2r_a^2/\omega_a^2)]$ is the aperture linear transmittance, r_a is the aperture radius, and ω_a is the beam radius at the aperture. The value of n_2 is evaluated using the following equation^[41]

$$n_2 = \frac{\Delta\phi}{KI_0L_{\text{eff}}}, \quad (2)$$

where $K = 2\pi/\lambda$ (λ is the laser wavelength), I is the beam intensity at the focus, $L_{\text{eff}} = [1 - \exp(-\alpha L)]/\alpha$ is the effective thickness of the sample depending on linear absorption coefficient (α), and L is the thickness of the sample. The n_2 of LPCC crystal is found to be $6.3 \times 10^{-11} \text{ cm}^2/\text{W}$. The TONLO absorption coefficient (β) is examined and evaluated using the open aperture Z-scan analysis. The open aperture Z-scan curve of LPCC crystal is shown in Fig. 3(b). It reveals that as the sample approaches to the focus point the intensity of transmitted light becomes low, which is the concrete evidence for the reverse saturable absorption (RSA) effect.^[48] In order to elaborate it, it must be realized that on a nanosecond time scale the existence of multiphoton absorption (MPA) and excited state absorption (ESA) phenomenon effectively reinforces the cross section of excited state absorption to capitalize the ground state absorption, which is the principle reason for the origin of RSA.^[49,50] The TONLO absorption coefficient (β) of grown crystal is evaluated from the following equation^[41]

$$\beta = \frac{2\sqrt{2}\Delta T}{I_0L_{\text{eff}}}, \quad (3)$$

where ΔT is the one valley value at the open aperture Z-scan curve. The β of LPCC crystal is found to be $7.29 \times 10^{-5} \text{ cm}/\text{W}$. The LPCC crystal with promising RSA property pronounces its liability for optical limiting devices.^[51,52] The TONLO susceptibility ($\chi^{(3)}$) is calculated using the following equations^[41]

$$\text{Re } \chi^{(3)} (\text{esu}) = 10^{-4}(\epsilon_0 C^2 n_0^2 n_2)/\pi (\text{cm}^2/\text{W}), \quad (4)$$

$$\text{Im } \chi^{(3)} (\text{esu}) = 10^{-2}(\epsilon_0 C^2 n_0^2 \lambda \beta)/4\pi^2 (\text{cm}/\text{W}), \quad (5)$$

$$\chi^{(3)} = \sqrt{(\text{Re } \chi^{(3)})^2 + (\text{Im } \chi^{(3)})^2}, \quad (6)$$

where ϵ is the vacuum permittivity, n is the linear refractive index of the sample, and c is the velocity of light in a vacuum. The knowledge of polarizing ability of crystal material at high power laser intensities is emphasized to be the most essential factor and the χ^3 is the parameter which gives the magnitude of polarizability in the material. The χ^3 of LPCC crystal is found to be 2.39×10^{-4} esu. The delocalization rate of charge transfer over the pi bonded network is the vital factor giving rise to large χ^3 .^[53]

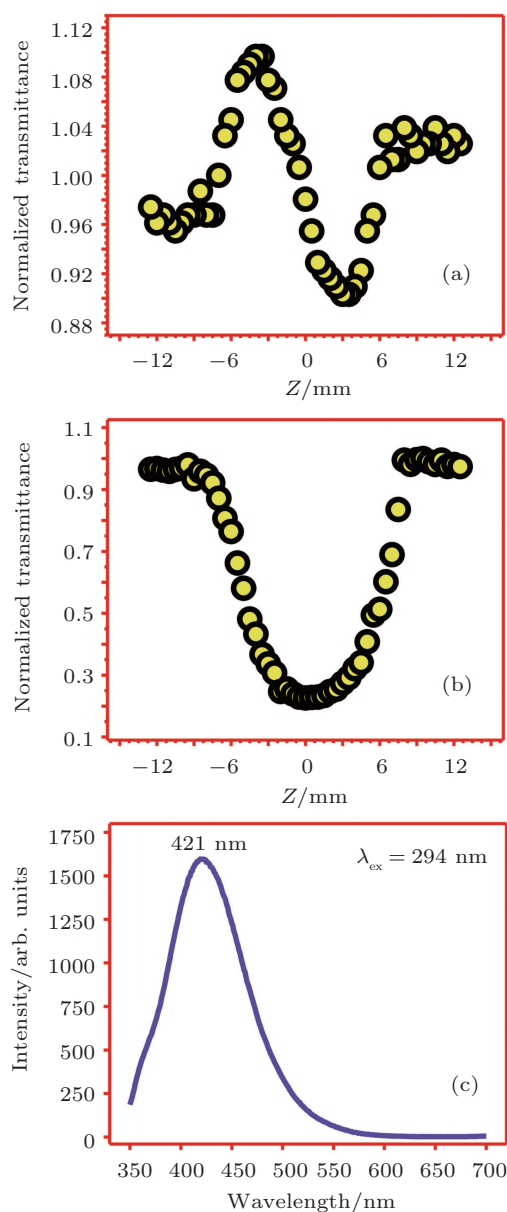


Fig. 3. (color online) Z-scan transmittance curve with aperture (a) closed and (b) open, (c) PL emission spectrum.

Photoluminescence (PL) is the most vital nondestructive technique that sufficiently unfolds the electronic band structures, transition tendency of electrons in different energy states, electronic purity of the material, and the disorders associated with alloys.^[54,55] The luminescence process involves the photo-excitation followed by photo-relaxation. The fluorophore (moiety of molecule responsible for its color) as-

sociated with the material is allowed to absorb the energy at the selected wavelength and re-emit the energy at a different but specific wavelength. The wavelength and intensity of emission relies on two factors: (i) the intrinsic nature of fluorophore and (ii) the surrounding environment of the fluorophore.^[56] The surrounding environment implicates the presence of dopant/defects/impurities, which majorly affects the trajectory of an electron during photo-relaxation.^[57] These aspects vitalize luminescence as a decisive feature which uncovers the exact property of the material. In the present analysis the luminescence study has been accomplished using the Hitachi FL-7000 spectrophotometer. Before the analysis, the instrument parameters were set to be excitation and emission slit width = 2.5 nm, scan speed = 240 nm/s, response time = 0.1 s, and delay = zero. The LPCC crystal material is photo-excited at an energy wavelength of 294 nm (4.22 eV) and the PL emission spectrum is recorded in a range of 350 nm–700 nm as shown in Fig. 3(c). It is observed that the LPCC crystal exhibits violet colored emission with high intensity and the peak maximum is centered at 421 nm. It is a known fact that the defects and impurities existing in a crystal avail more states for electrons and holes, which finally affects the transition energy, trajectory and lifetime of an electron.^[58] The absence of multiple peaks, smooth emission profile and high intensity of emission confirms that the LPCC crystal does not possess optically active defects and intermediate states. In the fields of biomedical, biochemical, and chemical research, the materials with unique emission behaviors are utilized to detect the compounds,^[59,60] and the LPCC crystal seems to meet the requirements for the discussed applications.

The dielectric measurement studies provide a great deal of information about the lattice dynamics and electric field distribution in material for exploiting the NLO applications.^[61] The dielectric constant and dielectric loss of LPCC crystal are evaluated at different temperatures (30 °C–80 °C) and frequencies (100 Hz, 1 kHz, 10 kHz, 100 kHz, 1 MHz) using the HIOKI-3532 LCR cubemeter. The response of the polarization mechanism (electronic, ionic, dipolar, and space charge) is the principle factor responsible for the dielectric constant in crystal material.^[62] The variation of the dielectric constant is shown in Fig. 4(a) and it is interesting to know that the dielectric constant of LPCC crystal increases with the increase in temperature but significantly decreases with the increase in frequency. It is due to the fact that all four polarizations are dominant at lower frequency and high temperature, which results in high magnitude of dielectric constant, on the contrary, the decrease in magnitude of dielectric constant is less at higher frequencies due to the diminished effect of foresaid polarizations.^[63] The space charge polarization plays an active role as the temperature of the material increases but as the frequency of applied field exceeds 1 kHz even the space charge

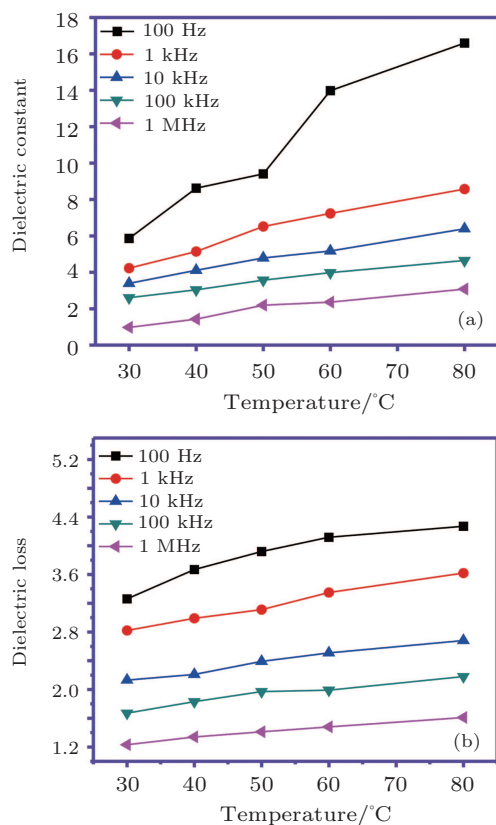


Fig. 4. (color online) Response of (a) dielectric constant and (b) dielectric loss.

polarization becomes deficient.^[64] It is an intruding observation that the LPCC crystal is reported to have a high dielectric constant in a given frequency range,^[19,65] however much lower, and the concurring results are obtained in the presently grown LPCC crystal, which might have stable growth at constrained temperature, high electronic purity and less hindrance of space charge polarization. It is highlighted that the dielectric constant of LPCC crystal has been tuned to much lower value as frequency increased to 1 MHz. The materials exhibiting low dielectric constant consume less power and offer decreased RC delay, which is vital for microelectronics devices^[66] and also enhances the SHG coefficient of the material.^[67] Thus the LPCC crystal with lower dielectric constant is considered to be a better alternative for fabricating photonics, electro-optic modulators, field detectors, THz wave generators, and microelectronic devices.^[68,69] The dissipation of electromagnetic energy in crystal medium is termed dielectric loss. The dielectric loss in single crystal is majorly contributed by macro/micro cracks, random crystal orientation, porosity, impurities, grain boundaries, etc.^[70,71] The response of dielectric loss shown in Fig. 4(b) reveals that the dielectric loss follows the same trend as that of the dielectric constant. The lower magnitude of dielectric loss at higher frequencies suggests that the LPCC crystal possesses a very small quantity of electrically active defects.^[72] It is noteworthy that the dielectric constant and dielectric loss show a lot less variation

at higher frequencies even when the temperature of the crystal sample is raised. From an application point of view the LPCC crystal could be a potential candidate for distinct technological devices.

4. Conclusions

LPCC bulk single crystal is successfully grown by the slow solvent evaporation technique. The EDS analysis confirmed the presence of constituent elements of LPCC crystal. In single crystal XRD analysis the LPCC crystal is found to have an orthorhombic crystal structure with space group $P2_12_12_1$. Linear optical studies employed within 200 nm–1100 nm reveal that the LPCC crystal has high optical transparency (84%), low cutoff wavelength (232 nm), wide optical band gap (5.35 eV), low refractive index, reflectance, extinction coefficient and increasing optical conductivity. The promising second and TONLO property of LPCC crystal is confirmed by Kurtz–Perry test and Z-scan analysis. The SHG efficiency of LPCC crystal is found to be 2.12 times higher than that of KDP crystal. The LPCC crystal possesses the negative nonlinear refraction and reverse saturable absorption under beam irradiation of wavelength 632.8 nm. The values of n_2 , β , and χ^3 of LPCC crystal are $6.3 \times 10^{-11} \text{ cm}^2/\text{W}$, $7.29 \times 10^{-5} \text{ cm/W}$, $2.39 \times 10^{-4} \text{ esu}$, respectively. The luminescence behavior investigated with 350 nm–700 nm confirms the prominence of violet colored emission in LPCC crystal with a maximum at 421 nm. The dielectric studies reveal that the dielectric constant and dielectric loss of LPCC crystal greatly decreases with the increase in frequency throughout the applied temperature range of 30 °C–80 °C. The LPCC crystal with high optical transparency, large SHG efficiency, promising TONLO properties, single colored emission, and low dielectrics advocates the efficient utility of LPCC crystal for applications in photonics, NLO, night vision sensors, biomedical, optical limiting, SHG, and microelectronics devices.

Acknowledgement

Author Mohd Anis extends his thanks to UGC, New Delhi, India for awarding Maulana Azad National Fellowship (Grant No. F1-17.1/2015-16/MANF-2015-17-MAH-68193). Author Ghramh H A expresses sincere gratitude to RCAMS-King Khalid University, Saudi Arabia for support. Authors are thankful to Prof. Kalainathan S, VIT University Vellore, India for extending the Z-scan facility. Dr. Das P K laboratory, IISc Bangalore is acknowledged for rendering the SHG test.

References

- [1] Wang X Q, Xu D, Lu M K, Yuan D R and Xu S X 2001 *Mater. Res. Bull.* **36** 879

- [2] He Y H, Lan Y Z, Zhan C H, Feng Y L and Su H 2009 *Inorg. Chem. Acta* **362** 1952
- [3] Verbiest T, Houbrechts S, Kauranen M, Clays K and Persoons A 1997 *J. Mater. Chem.* **7** 2175
- [4] Lu G W, Xia H R, Wang X Q, Xu D, Chen Y and Zhou Y Q 2001 *Mater. Sci. Eng. B* **87** 117
- [5] Sugandhi K, Verma S, Jose M, Joseph V and Das S J 2013 *Opt. Laser Technol.* **54** 347
- [6] Peter M E and Ramasamy P 2010 *J. Cryst. Growth* **312** 1952
- [7] Hanumantharao R and Kalainathan S 2012 *Mater. Lett.* **74** 74
- [8] Liu X J, Xu D, Wei X Q, Ren M J and Zhang G H 2010 *Mater. Sci. Eng. B* **166** 203
- [9] Bright K C and Freeda T H 2010 *Physica B* **405** 3857
- [10] Sethuraman K, Babu R R, Gopalakrishnan R and Ramasamy P 2008 *Cryst. Growth Des.* **8** 1863
- [11] Shkir M, Alfaify S, Ajmal Khan M, Dieguez E and Perles J 2014 *J. Cryst. Growth* **391** 104
- [12] Arockia Avila S, Selvakumar S, Francis M and Rajesh A L 2017 *J. Mater. Sci. Mater. Electron.* **28** 1051
- [13] Maadeswaran P and Chandrasekaran J 2011 *Optik* **122** 1128
- [14] Boopathi K, Jagan R and Ramasamy P 2016 *Appl. Phys. A* **122** 689
- [15] Raj C J and Das S J 2008 *Cryst. Growth Des.* **8** 2729
- [16] Anbuselvi D, Theras J E M, Jayaraman D and Joseph V 2013 *Physica B* **423** 38
- [17] Kandasamy A, Siddeswaran R, Murugakoothan P, Kumar P S and Mohan R 2007 *Cryst. Growth Des.* **7** 183
- [18] Prakash J T J and Kumararaman S 2008 *Mater. Lett.* **62** 4097
- [19] Shkir M, Kushwaha S K, Maurya K K, Bhatt R C, Rashmi, Wahab M A and Bhagavannarayana G 2010 *Mater. Chem. Phys.* **120** 566
- [20] Singh P, Hasmuddin M, Shkir M, Vijayan N, Abdullah M M, Ganesh V and Wahab M A 2013 *Mater. Chem. Phys.* **142** 154
- [21] Sun Z H, Xu D, Wang X Q, Zhang G H, Yu G, Zhu L Y and Fan H L 2009 *Mater. Res. Bull.* **44** 925
- [22] Sivakumar N, Kanagathara N, Varghese B, Bhagavannarayana G, Gunasekaran S and Anbalagan G 2014 *Spectrochem. Acta A* **118** 603
- [23] Shaikh R N, Anis M, Shirsat M D and Hussaini S S 2014 *J. Optoelectron. Adv. Mater.* **16** 1147
- [24] Kakani S L and Kakani A 2004 *Material Science* (New Delhi: New Age International) p. 417
- [25] Anis M, Ramteke S P, Shirsat M D, Muley G G and Baig M I 2017 *Opt. Mater.* **72** 590
- [26] Weber M J 2003 *Handbook of Optical Materials* (New York: CRC Press)
- [27] Bass M 1995 *Handbook of Optics*, Volume 2 (USA: Mc-Graw Hill) p. 33.12
- [28] Ramteke S P, Baig M I, Shkir M, Kalainathan S, Shirsat M D, Muley G G and Anis M 2018 *Opt. Laser Technol.* **104** 83
- [29] Ganapayya B, Jayarama A, Sankolli R, Hathwar V R and Dharmaparakash S M 2012 *J. Mol. Struct.* **1007** 175
- [30] Anis M, Pandian M S, Baig M I, Ramasamy P and Muley G G 2017 *Mater. Res. Innov.*
- [31] Sangeetha K, Prasad L G and Mathammal R 2016 *Physica B* **501** 5
- [32] Rajagopalan N R and Krishnamoorthy P 2017 *J. Inorg. Organomet. Polym. Mater.* **27** 296
- [33] Anis M and Muley G G 2016 *Phys. Scr.* **91** 85801
- [34] Chen C T and Liu G Z 1986 *Ann. Rev. Mater. Sci.* **16** 203
- [35] Schubert E F, Kim J K and Xi J Q 2007 *Phys. Stat. Sol. B* **244** 3002
- [36] Raja M V A, Anand D P and Madhavan J 2013 *Sci. ActaXaveriana* **4** 41
- [37] Kurtz S K and Perry T T 1968 *J. Appl. Phys.* **39** 3698
- [38] Wojciechowski A, Alzayed N, Kityk I, Berdowski J, and Tylczyński Z 2010 *Opt. Appl.* **XL** 1007
- [39] Pahrkar V G, Anis M, Baig M I, Ramteke S P and Muley G G 2017 *Optik* **142** 421
- [40] Li Y, Wang M, Zhu T, Meng X, Zhong C, Chen X and Qin J 2012 *Dalton Trans.* **41** 763
- [41] Bahae M S, Said A A, Wei T H, Hagan D J and Stryland E W V 1990 *IEEE J. Quantum Electron.* **26** 760
- [42] Baig M I, Anis M, Kalainathan S, Babu B and Muley G G 2017 *Mater. Technol. Adv. Perform. Mater.* **32** 560
- [43] Gu B, Wang H T and Ji W 2009 *Opt. Lett.* **34** 2769
- [44] Ramteke S P, Anis M, Pandian M S, Kalainathan S, Baig M I, Ramasamy P and Muley G G 2018 *Opt. Laser Technol.* **99** 197
- [45] Sun X B, Wang X Q, Ren Q, Zhang G H, Yang H L and Feng L 2006 *Mater. Res. Bull.* **41** 177
- [46] Rasal Y B, Anis M, Shirsat M D and Hussaini S S 2017 *Mater. Res. Innov.*
- [47] Muthuraja A and Kalainathan S 2017 *Mater. Technol. Adv. Perform. Mater.* **32** 335
- [48] Azhar S M, Anis M, Hussaini S S, Kalainathan S, Shirsat M D and Rabbani G 2016 *Mater. Sci. Poland* **34** 800
- [49] Zhang Y D, Zhao Z Y, Yao C B, Yang L, Li J and Yuan P 2014 *Opt. Laser Technol.* **58** 207
- [50] Zidana M D, Al-Ktaifani M M and Allahham A 2017 *Opt. Laser Technol.* **90** 174
- [51] Azhar S M, Hussaini S S, Shirsat M D, Rabbani G, Shkir M, AlFaify S, Ghramh H A, Baig M I and Anis M 2017 *Mater. Res. Innov.*
- [52] Kumar R S S, Rao S V, Giribabu L and Rao D N 2007 *Chem. Phys. Lett.* **447** 274
- [53] Shaikh R N, Anis M, Shirsat M D and Hussaini S S 2018 *Optik* **154** 435
- [54] Anis M, Hussaini S S, Shirsat M D, Shaikh R N and Muley G G 2016 *Mater. Res. Express* **3** 106204
- [55] Anis M, Baig M I, Pandian M S, Ramasamy P, AlFaify S, Ganesh V, Muley G G and Ghramh H A 2018 *Cryst. Res. Technol.*
- [56] Sauer M, Hofkens J and Enderlein J 2011 *Handbook of Fluorescence Spectroscopy and Imaging* (Weinheim: Wiley-VCH)
- [57] Chandran S, Paulraj R and Ramasamy P 2015 *Mater. Res. Bull.* **68** 210
- [58] Timothy H G 2000 *Photoluminescence in analysis of surfaces and interfaces*, in *Encyclopedia of Analytical Chemistry* (Chichester: John Wiley & Sons) p. 9209
- [59] Kajamuhideen M S, Senthuraman K, Ramamurthi K and Ramasamy P 2017 *Opt. Laser Technol.* **91** 159
- [60] Shaikh R N, Anis M, Shirsat M D and Hussaini S S 2015 *Mater. Technol. Adv. Perform. Mater.* **19** 187
- [61] Subhashini R, Sathya D, Sivashankar V, Mageshwari P S L and Arjunan S 2016 *Opt. Mater.* **62** 357
- [62] Riscob B, Shkir M, Sundar J K, Natarajan S, Wahab M A and Bhagavannarayana G 2011 *Spectrochem. Acta A* **78** 543
- [63] Anis M, Muley G G, Baig M I, Hussaini S S and Shirsat M D 2017 *Mater. Res. Innov.* **21** 439
- [64] Singh P, Hasmuddin M, Abdullah M M, Shkir M and Wahab M A 2013 *Mater. Res. Bull.* **48** 3926
- [65] Kandasamy A, Mohan R, Caroline M L and Vasudevan S 2008 *Cryst. Res. Technol.* **43** 186
- [66] Hatton B D, Landskron K, Hunks W J, Bennett M R, Shukaris D, Perovic D D and Ozin G A 2006 *Mater. Today* **9** 22
- [67] Miller R C 1964 *Appl. Phys. Lett.* **5** 17
- [68] Jazbinsek M, Mutter L and Gunter P 2008 *IEEE J. Sel. Top. Quantum Electron.* **14** 1298
- [69] Anis M, Muley G G, Pahrkar V G, Baig M I and Dagdale S R 2018 *Mater. Res. Innov.* **22** 99
- [70] Jiang M H and Fang Q 1999 *Adv Mater.* **11** 1147
- [71] Baig M I, Anis M and Muley G G 2017 *Opt. Mater.* **72** 1
- [72] Ramteke S P, Anis M, Baig M I and Muley G G 2018 *Optik* **154** 275